Journal of Electronics, Electromedical Engineering, and Medical Informatics
Homepage: jeeemi.org; Vol. 7, No. 3, July 2025, pp: 940-949 **e-ISSN: 2656-8632**

RESEARCH ARTICLE OPEN ACCESS

Machine Learning-Based Approach for Uterine Cancer Detection and Classifier Evaluation

Brindha Samarasam[1, 2] and Judith Justin[1]

[1] Department of Biomedical Instrumentation Engineering, Avinashilingam Institute for Home Science and Higher Education for Women, Coimbatore, India
[2] Department of Electronics and Communication Engineering, Nandha Engineering College,Erode, India
Corresponding author: Brindha Samarasam (e-mail: brindha.bliss@gmail.com**)**

Abstract **The necessity of early diagnosis of abnormal cell growth is critical to support patient monitoring and earlier clinical analysis. Uterine cancer is the most common gynecological malignancy among women, with endometrial cancer being the predominant type occurring in the endometrial layer. Endometrial cancer is a commonly identified type of uterine cancer that majorly occurs in the endometrial layer. This research applies machine learning (ML) algorithms to detect uterine cancer using texture-based features extracted from medical images. Specifically, a hybrid combination of Grey Level Co-occurrence Matrix (GLCM) and Grey Level Run Length Matrix (GLRLM) properties is proposed to derive 34 features, including entropy, long-run emphasis, short-run low grey level emphasis, and high grey level run emphasis. To ensure data quality, a comprehensive dataset was collected and preprocessed, followed by the implementation of an improved approach for feature normalization and ranking . The top-ranked features were then used to train and validate multiple ML algorithms, including Adaptive Neuro-Fuzzy Inference System (ANFIS), K-Nearest Neighbor (K-NN), Linear Discriminant Analysis (LDA), Radial Basis Function (RBF), Support Vector Machine (SVM), Naïve Bayes (NB), and Artificial Neural Network (ANN). Results show that the best-performing algorithm achieves an accuracy of 97.3%, sensitivity of 96.3%, and specificity of 99.2%. The algorithm's performance was further validated using Receiver Operating Characteristics (ROC) analysis and F1 scores, both of which demonstrated superior predictive capability. Additionally, Explainable AI (XAI) techniques were integrated to elucidate the features and patterns recognized by the algorithm as indicative of endometrial carcinoma. Layer-wise relevance propagation (LRP) was employed to backtrack the neural network's output decisions to the input features, highlighting the most influential factors in the algorithm's predictions. This research demonstrates the potential of applying ML algorithms to improve early detection of uterine cancer, offering a non-invasive, accurate, and cost-effective alternative to traditional imaging methods.**

Keywords **ANN, ANFIS, GLCM, GLRLM, KNN, LDA, NB, RBF, SVM, Uterine Cancer, XAI**

I. Introduction

Radio waves and magnets used to capture images inside of the human body are executed with the highest level of accuracy through Magnetic Resonance Imaging (MRI) modality. Soft tissues such as muscles and organs can be visualized without any obstructions from bones. MRI is also considered as the most effective method for evaluating and detecting abnormal cell behavior in the uterus [1]. The incidence of endometrial carcinoma in the female genital tract is estimated at approximately 25 cases per 100,000 women, as indicated by data from the Surveillance, Epidemiology, and End Results (SEER) program. This is a leading malignant tumor found mainly in industrialized countries. For treatment planning, MRI is the preferred imaging modality due to its superior capabilities. Staging analysis using MRI typically involves major findings such as the depth of myometrial invasion, lymph node metastases, and cervical extension [2]. Preoperatively, various imaging techniques, including Magnetic Resonance Imaging, Transvaginal Ultrasonography (TVUS), and Computed Axial Tomography, are employed to identify the status of uterine or endometrial carcinoma[3]. Though ultrasound is often used in initial findings, its sensitivity and specificity for detecting carcinoma are 96% and 61% respectively, in a postmenopausal woman having an endometrial thickness of 5 mm [4]. However, delineating the margins of the tumor using ultrasound is very difficult, and majorly produces negative

Manuscript received 22November 2024; Revised 10 March 2025; 10 June 2025; Accepted 15 July 2025; Available online 30July 2025
Digital Object Identifier (**DOI**): https://doi.org/10.35882/jeeemi.v7i3.632

Journal of Electronics, Electromedical Engineering, and Medical Informatics
Homepage: jeeemi.org; Vol. 7, No. 3, July 2025, pp: 940-949 **e-ISSN: 2656-8632**

predictive value for the thin endometrial layer[5]. Additionally, TVUS has a limited field of view, which is another drawback. Various other limitations include difficulty in detecting lymphovascular space invasion, and estimating the extent of myometrial invasion in the presence of large tumors. The data for predicting parametrical invasion, cervical extension, is insufficient while using the TVUS imaging modality[6]. Similarly, computed tomography is less reliable for identifying myometrial invasion, with sensitivity ranging from 40% to 80% and specificity between 40% and 75%. In contrast to the limitations of TVUS and CT, MRI provides the most accurate pre-treatment local staging and secondary tissue delineation [7]. This study aims to develop an AI-driven approach to identify and classify Uterine Corpus Endometrial Carcinoma (UCEC) using machine learning. By incorporating Explainable AI (XAI), the model's decisions-making process becomes more transparent, ensuring clinicians trust and effectively use the system in real-world diagnosis.

The most prevalent gynecological malignancies of the female reproductive system are uterine cancer, particularly endometrial carcinoma. Early diagnosis of cancerous cells remains a challenge because of limitations in imaging modalities and parametric measures that process t tumor boundaries and the invasion of cancerous cells into the myometrial layer later. While MRI offers better soft tissue contrast, interpretation by radiologists mya introduce variability and delays in diagnosis. In recent years, the field of medical image analysis has witnessed significant progress, particularly in the automatic classification of normal and abnormal subjects using various machine learning (ML) and deep learning (DL) techniques for assisting in the classification of Uterine cancer[8]. This automated process is pivotal for the early assessment of degenerative diseases affecting the uterus. A new geometric feature, selected through recursive feature elimination, has been employed in predictive models. A new Ensemble method[9], ResNet have been employed to support radiologists in staging and lesion identification. Methods like geometric [10],radiomic [11], [12], and deep features for classification were used, yet they achieved better accuracy, low interpretability. Reducing high complexity in real-world settings is a study. This research proposes a hybrid feature extraction approach combining GLCM and GLRLM texture features, forming a Hybrid feature set. The extracted features are subjected to normalization and a ranking procedure, followed by classification. Layer-wise Relevance Propagation is used to backtrack and enhance transparency. This work aims to develop an interpretable, noninvasive method for the detection and classification of uterine cancer using machine learning models powered with Explainability. The contribution includes 1) Development of a hybrid feature set, 2) Introducing a novel ranking method based on statistical range differences, and 3) Enhancing Model Transparency for Clinicians, making it easier for healthcare professionals to understand how decisions are made, thereby increasing trust in AI-driven tools. Bridging the Gap Between AI and traditional machine learning descriptors for Clinical Decision-Making.

This study is structured as follows: Section II reviews related works and recent advances in uterine cancer classification. Section III describes the materials and proposed methodology, including preprocessing, feature extraction, normalization, ranking, and classification. Section IV presents the experimental results and evaluation metrics. Section V discusses classifier comparisons, XAI integration, and performance implications. Section VI concludes the work with a summary of findings and directions for future research.

II. Related Works

Yasunari Fujinaga *et al*. evaluates radiomic machine learning classifiers based on multiparametric MRI for the assessment of risk factors in endometrial carcinoma. Radiomic features were extracted from T2-weighted images, apparent diffusion coefficient maps, and contras-enhanced T1-weighted images. Various classifiers were built to predict histological grade, lymphovascular invasion, etc. The mean AUC values for these machine learning classifiers indicated better diagnostic procedures. These classifiers support the pre-treatment assessment of endometrial carcinoma risk factors. Integration of machine learning into clinical practices improves the diagnostic procedure with the assistance of machine learning [13]. Pier Paolo Mainenti *et al*. suggested a machine learning-based approach for stratifying endometrial cancer patients. Three-dimensional T2-weighted MRI images were used to obtain the tumor volume of interest. Various radiomic features were extracted using a Pyradiomics-based pipeline and were involved in a rigorous feature selection process, which also included feature stability, variance, and pairwise correlation. A Support Vector machine algorithm for risk stratification was developed, achieving an accuracy of 0.71 in the training datasets[14], [15]. This work addresses the existing gap in the literature by focusing on texture-based feature extraction using Grey Level Co-occurrence Matrix (GLCM) and Grey Level Run Length Matrix (GLRLM) properties for uterine cancer detection, particularly for identifying endometrial carcinoma. Unlike previous studies that primarily utilized radiomic or geometric features, this approach emphasizes rigorous preprocessing, normalization, and feature

Manuscript received 22November 2024; Revised 10 March 2025; 10 June 2025; Accepted 15 July 2025; Available online 30July 2025
Digital Object Identifier (**DOI**): https://doi.org/10.35882/jeeemi.v7i3.632

ranking to ensure data quality and optimize machine learning model performance.

III. Methods

A. Dataset

The dataset used in this research consists of 1398 Magnetic Resonance Imaging (MRI) scans of the uterus. These images are categorized as either normal or abnormal. Among them, 916 images represent normal cases, while 482 correspond to abnormal cases. Each image was taken in DICOM format, with consistent resolution and parameters suitable for quantitative analysis. The dataset was split into training and testing sets using a 4:1 ratio.

B. Data Collection

The images were sourced from the Cancer Imaging Archive, a publicly available database for medical imaging research. The dataset consists of 1,398 MRI scans of the uterus, which were divided into training, validation, and testing subsets to ensure a structured and comprehensive evaluation of the model. Approximately 70% of the dataset (979 images) was allocated for the training phase, allowing the model to learn effectively from the majority of the available data. To fine-tune and monitor the model's performance during training, 15% of the dataset (210 images) was designated as the validation set. The remaining 15% (209 images) was set aside as the testing set to evaluate the model's predictive capability on unseen data after the training and validation stages were completed.

C. Data Processing

In the forum of medical image diagnostics, the proposed system is dedicated for early uterine cancer detection through the analysis of Uterine Magnetic Resonance Imaging (MRI) scans. The methodology begins with a denoising process utilizing a bilateral filter, ensuring image clarity and precision of MRI images. Machine Learning Techniques such as the Grey Level Co-occurrence Matrix (GLCM) transformation and the collective combination of GLCM and Grey Level Run Length Matrix (GLRLM) for feature extraction, support in understanding uterine tissue characteristics [16]. The overall block diagram of the proposed methodology for detecting uterine cancer using the Adaptive Neuro Fuzzy Inference System classifier is shown in Fig. 1. The feature selection is followed by focusing on and identifying the most pertinent aspects for precise classification. The system incorporates the Adaptive Neuro Fuzzy Inference System (ANFIS) classifier, a dynamic and adaptive artificial intelligence component trained on the selected features[17]. Magnetic Resonance Imaging (MRI) technology, which supports capturing images of internal organs using magnetic field gradients, is generally affected by various types of noises such as salt and pepper noise, Gaussian noise, speckle noise, Rayleigh noise, Rican noise, etc. Removing these noises from the MR images is essential for further diagnostic procedures. A bilateral filter is one of the conventional filters used for image denoising. A bilateral filter is generally called an edge-preserving filter and supports the noise reduction process. It also acts as a smoothing filter for images and is nonlinear. The grey value of each pixel is replaced with a weighted average of the grey values of neighboring pixels based on the Gaussian distribution. The weight does not limit the Euclidean distance of the pixels but extends to radiometric variations such as color intensity, range difference, and depth distance. It supports preserving the sharp edges. Denoising the intensity of a pixel is achieved by calculating the weights and normalizing them [18]. Feature Extraction is an essential procedure in differentiating the carcinoma-identified uterus image from normal uterus images. It is the procedure by which texture features within the image are extracted for further processing in the decision-making process. Various texture features were extracted from the pre-processed image based on GLCM and GLRLM. The combination of repeated patterns occurring frequently in the region of interest of an image is termed texture. The texture models were generated using the Hybrid Feature Set (HFS), which combines GLCM and GLRLM texture properties. The GLCM-based feature extraction is a second-order statistical method of examining an image's texture that considers the spatial relationship between two pixels. The GLCM function categorizes the texture of an image by computing the frequently occurring pixel pair with intensity value 'r' that appears in any of the horizontal, vertical, or diagonal forms to the adjacent pixels with the value 'c'((r,c) represents the intensity values in the image) as shown in Eq. (1)[19].

$$\sum\sum P(r,c \mid \theta) \text{ and, } 1 \leq \mathrm{Nx}(\theta) \leq \mathrm{Ny} \quad (1)$$

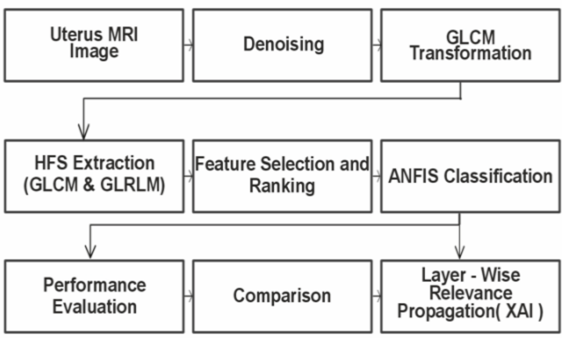

Fig. 1. Block Diagram of Uterus cancer identification using ANFIS with Hybrid Feature Set

Manuscript received 22November 2024; Revised 10 March 2025; 10 June 2025; Accepted 15 July 2025; Available online 30July 2025
Digital Object Identifier (**DOI**): https://doi.org/10.35882/jeeemi.v7i3.632

Journal of Electronics, Electromedical Engineering, and Medical Informatics
Homepage: jeeemi.org; Vol. 7, No. 3, July 2025, pp: 940-949 **e-ISSN: [2656-8632](https://issn.org)**

where, N_i is the Grey values in the image, N_l is the Run length of the pattern, and Ny is considered as the Total pixels in the image. Nx(θ) is the Number of N_la long angle θ; P(r,c|θ) is the Run length matrix for an arbitrary direction θ. Fig. 2 shows the flow chart of the proposed method for finding uterine cancer using ANFIS with HFS. The various texture features obtained from the images, like correlation, entropy, etc., are computed using the texture matrix. Table1shows the high-order statistical features of an MRI uterus image extracted using the GLRLM method.

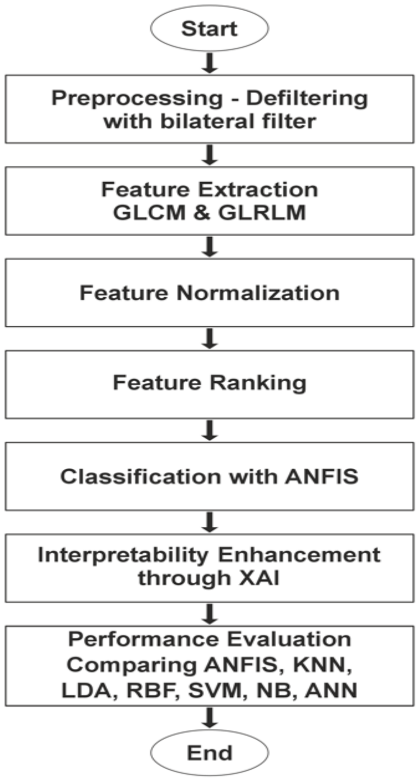

Fig. 2. Flow chart for finding Uterus cancer using ANFIS with Hybrid Feature Set.

GLRLM a two-dimensional histogram represented by a matrix. All the combinations of grey level values and grey level runs, in particular the direction of ROI, represent its occurrence. The relationship and distribution of an image pixel are measured to extract the statistical features of the MR imaging modality. The group of continuous pixels has the same intensity level. At the same time, the run length denotes the number of neighborhood intensity levels in a specific direction. This value is computed by counting the frequently occurring runs in the MRI image. The r, c element in the GLRLM matrix P(r, c)|θ indicates the number of runs with intensity level 'r' and length 'c' occurring in the image of angle θ.

Table 1. Extracted Feature values for an MRI Uterus image (Sample)

Features	Value
Uniformity / Energy / Angular Second Moment (done)	0.02549
Entropy	0.27207
Dissimilarity	4.07772
Contrast	58.2975
Inverse difference	0.39899
correlation	0.98736
Homogeneity / Inverse difference moment	0.24712
Autocorrelation	0.94000
Cluster Shade	0.18052
Cluster Prominence	0.99261
Maximum probability	0.99152
Information measures of correlation (1)	0.06554
Information measures of correlation (2)	-0.69247
Maximal correlation coefficient	0.42512
Inverse difference normalized (INN)	0.99663
Inverse difference moment normalized (IDN)	0.99740
Inertia	62.22051
Long Runs Emphasis	0.14010
Short Runs Emphasis	0.94408
Gray Level Non- uniformity	0.94408
Run Length Non-uniformity	0.817500
Run Percentage	0.8754
Low Gray Level Run Emphasis	0.02855
High Gray Level Run Emphasis	0.94081
Short Run Low Gray Level Emphasis	0.622110
Short Run High Gray Level Emphasis	0.27207
Long Run Low Gray Level Emphasis	0.88731
Long Run HighGray Level Emphasis	0.88731

The extracted features are normalized to a single scale. The feature extraction process is carried out using the HFS algorithm, while feature normalization is not essential for the ANFIS classifier. It is observed that while considering the actual feature values, the time complexity increases. The process of optimization reduces this drawback to about 25% of the total time complexity. The Min-Max algorithm is used to normalize the features on a single scale. Different ranges of the feature values obtained are rescaled between 0 and 1 with the modified Min-Max algorithm.

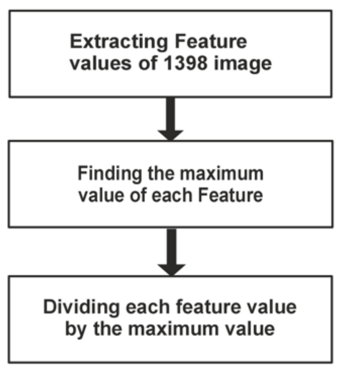

Fig.3. Feature normalization procedure

Manuscript received 22November 2024; Revised 10 March 2025; 10 June 2025; Accepted 15 July 2025; Available online 30July 2025
Digital Object Identifier (**DOI**): https://doi.org/10.35882/jeeemi.v7i3.632

The preferred scale limits are set to a minimum of 0 and a maximum of 1. Consider the feature values as F1, F2, F3...FN. The algorithm for feature normalization is shown in Fig. 3. Finding the maximum value of each feature.

$$Fimax = max\,[\,FiI1, FiI2, Fi3, \ldots FiIn] \quad (2)$$

$$Fimax = max[Fik]_{k=I1}^{k=In} \quad (3)$$

where k is the image ranging from i_1 to i_n. Dividing each feature value by the maximum value

$$F\text{ Norm} = \frac{FiIn}{max[Fik]_{k=I1}^{k=In}} \quad (4)$$

FNorm is the Feature Normalization, and I is number of features. The maximum value of each feature is calculated from t Eq. (2) and Eq. (3). The calculated maximum feature value is divided for normalization from Eq (4)[20]. The best precision value is achieved by considering the feature values in the floating-point formats shown in tTable 2. The Feature Ranking and Selection Algorithm is an essential process in optimizing the feature set for uterine MRI image classification.

Table 2. Feature normalization

Step	Instruction
1	The feature values are denoted by F1, F2, F3…F34.
2	All 34 features are extracted for 1398 images (916 Normal and 482 Abnormal).
3	The maximum value for each column is calculated.
4	Each value is divided by the maximum value of the corresponding column.
5	All the values in the table vary between the ranges 0 and 1.

Fig.4 shows the Proposed Feature Ranking Procedure for selecting the best performing features among 34 texture features in the Hybrid Feature Set as shown in Table 3. Following the Feature Normalization procedure, the algorithm calculates the maximum and minimum values for each of feature across all 1,398 images. It then computes the difference between these values, indicating the variability of each feature.

Table 3. Feature Ranking Algorithm

Step	Instruction
1	Step 1-5 from the Feature Normalization procedure.
6	Calculate the maximum and Minimum value of each column .
7	Compute the difference between the minimum and maximum value of each column.
8	Rearrange columns in descending order based on the computed differences
9	Select the required number of top-ranked features.

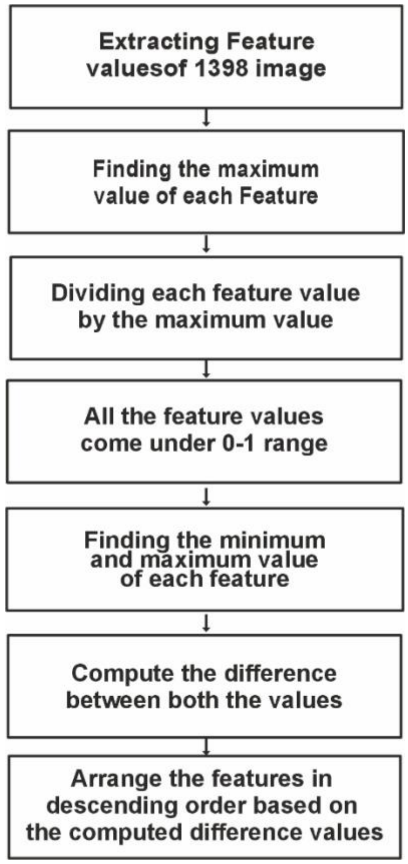

Fig. 4. Feature Ranking procedure

The columns are rearranged in descending order based on these variability, emphasizing the importance of each feature. The algorithm selects the required number of top-ranked features , ensuring that the most influential features are prioritized. By prioritizing features with higher variability, the algorithm enhances the discriminative power of the feature set, ultimately contributing to the improved performance of the Adaptive Neuro Fuzzy Inference System (ANFIS) classifier in uterine MRI image classification.

2. Result

A. Performance

The hybrid feature set, consisting of GLRLM and GLCM features, was extracted from the preprocessed MRI images. The extracted features were then used during the training phase of the Neuro fuzzy Classifier . After the training process, the Neuro fuzzy classifier generates a "fuzzy inference system," which classifies images as normal and abnormal . The accuracy

Manuscript received 22November 2024; Revised 10 March 2025; 10 June 2025; Accepted 15 July 2025; Available online 30July 2025
Digital Object Identifier (**DOI**): https://doi.org/10.35882/jeeemi.v7i3.632

Journal of Electronics, Electromedical Engineering, and Medical Informatics
Homepage: jeeemi.org; Vol. 7, No. 3, July 2025, pp: 940-949 e-ISSN: 2656-8632

increases using the hybrid feature set to classify the uterus images. The parameters of ANFIS collectively govern the architecture and behavior of the ANFIS model, as shown in Table 4, allowing it to adapt and learn from input-output patterns in a fuzzy rule-based framework it as given below [20]. Number of membership functions per input is 3, and three membership functions per input feature for moderate granularity. The type of MFs is Gaussian, the Gaussian-shaped membership functions for smooth and continuous modeling. Number of Rules is 25, which is a moderate number of fuzzy rules to capture complex relationships. Learning Algorithm such as Hybrid (Gradient Descent and Back propagation) Combines gradient descent and back propagation for efficient learning. Epochs are 100, and the Number of training iterations for adjusting parameters. Error and Tolerance, Mean Squared Error (MSE) with Tolerance 0.001, and Training stops when the mean squared error falls below 0.001. Input/output Scaling Factors are Auto and automatically scale input and output data. Initial FIS Parameters is Random and Random initial values for FIS parameters before training.

Table 4. Performance Metrics value of various Classifiers

Classifiers/ Metrics	PPV	NPV	Sensitivity	Specificity	Accuracy	F1-Score
KNN[21]	85.8	97.6	99.1	68.9	88.7	91.97
LDA[22]	90.8	98	99.1	80.9	92.8	94.77
RBF[23]	95.3	95.2	97.6	90.9	95.3	96.44
SVM[9]	95.1	96.5	98.3	90.5	95.6	96.67
NB [24]	96.5	95.3	97.6	93.4	96.1	97.05
ANN [25]	97	95	97.4	94.2	96.3	97.20
Proposed ANFIS	99.5	93.4	96.3	99.2	97.3	97.87

The type of Sugeno Inference System is First-Order. Utilizes a first-order Sugeno fuzzy model for output generation. Consequent Parameters is Linear and Linear coefficients in the consequent part of fuzzy rules. This split ensures a balanced training, validation, and testing approach, thereby improving the model's generalization ability. Fig.5 shows the Normal uterine image and an abnormal uterine MRI image classified as an abnormal uterine carcinoma image. The normal image anatomy appears with typically no abnormality or lesion found. Axial T2-weighted MRI image of the uterus in a healthy subject.

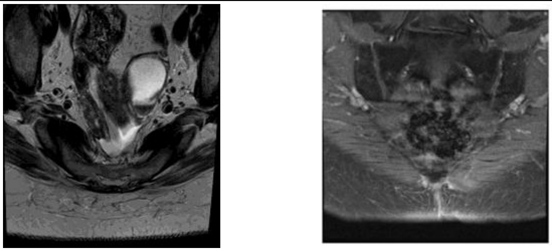

(a) (b)

Fig.5. Uterine MRI image (a) normal, (b) abnormal

In the normal image (a), the uterine contours are smooth and well defined. The endometrial strip is uniform thickness, and the myometrium shows proper homogeneous signal intensity. There is no evidence of abnormal mass, fluid collection, or structural distortions. In contrast, the abnormal image (b) is an axial T2-weighted MRI image of a uterus diagnosed with endometrial carcinoma. The endometrium appears abnormally thick, with heterogeneously hyperintense lesion occupying the endometrial cavity. The image was labeled as abnormal based on the radiological diagnosis of endometrial carcinoma. It exhibits distinguishing features from the normal anatomy, which is challenging for training and testing the machine learning model. The image was used as a part of an abnormal class during development and evaluation in the classification task.

3. Discussion

A. Classifier Performance Comparison

A comprehensive comparison with similar studies reveals a range of techniques employed in similar studies, focusing on detecting endometrial carcinoma. Xueliangzhu *et al.* propose a computer-aided method for detecting the deep myometrial invasion in the endometrial cancer MRI image. The method used corpus uteri region without considering any segmentation. A novel geometric feature, the linearity score, that captures the irregularities caused by cancer. The extracted texture features were refined using recursive feature elimination. These features are classified using an ensemble probabilistic SVM model with an accuracy of 93.7%, sensitivity of 94.7%, specificity of 93.3% and F1 Score of 87.8% demonstrating that the combination of geometric and texture features enhances the predictive strength for decision making. These performance metrics, when compared with the proposed work, have their own variations in the values accordingly[9].

Gabriel Levin *et al.* performed a study involving 160 endometrial intra epithelial neoplasis patients using machine learning models. A total of 48 models were evaluated with varying parameters. The performance of each model was assessed based on sensitivity,

Manuscript received 22November 2024; Revised 10 March 2025; 10 June 2025; Accepted 15 July 2025; Available online 30July 2025
Digital Object Identifier (DOI): https://doi.org/10.35882/jeeemi.v7i3.632

Journal of Electronics, Electromedical Engineering, and Medical Informatics
Homepage: jeeemi.org; Vol. 7, No. 3, July 2025, pp: 940-949 e-ISSN: 2656-8632

specificity, and Area under the curve, where a fivefold cross-validation was used, and mean metrics were evaluated, showing the result of 71% to 88 % for specificity ,while sensitivity remained low, showing 23% to 51%. The logistic regression model achieved the highest specificity of 88 % and the random forest had the highest AUC of 0.646, showing limited accuracy. Comparing with the proposed work shows an outperforming outcome comparatively [10].

Pier Paolo Mainenti *et al.* performed a study on 133 patients with endometrial carcinoma, including a feature selection process based on stability analysis, low variance removal, inter-feature correlation assessment, and recursive feature elimination. Support Vector Machine classifier was developed using two-fold cross validation, achieving an accuracy of 71% on the training set and 72 % on the testing set showing a reliable result. On comparing with the proposed work the SVM has proven to be an outperforming result in various performance metrices measured [14]. Wei Deng et al. performed a systematic review and meta-analysis on 45 MRI-based methodologies using radiomics quality score proving 13.77 with an acceptable range of 9 to 22.5, ranging between a moderate quality, showing that the proposed method proves in various dimensions of results extracted[15]. Nallasivan *et al.* proposed an automated system for brain tumor detection from MRI images, integrating multiple image processing and machine learning techniques. Tumor segmentation was performed using Fuzzy C-means clustering algorithm. Feature extraction was performed using the gray level co-occurrence Matrix with features including energy, contrast, homogeneity, entropy, and correlation. These features were fed to various classifiers, including Artificial Neural Network ANN, compared with SVM, KNN, Back propagation, and ANFIS, achieving accuracy of 95.7%,sensitivy of 98.5% and specificity of 95% which supports the proposed system for endometrial classification using machine learning algorithms [7].

The Adaptive Neuro Fuzzy Inference System classifier is compared with existing machine learning classifiers such as, K-Nearest Neighbor (K-NN), Linear Discriminant Analysis (LDA), Radial Basis Function (RBF), Support Vector Machine (SVM), Naïve Bayes (NB), and Artificial Neural Network (ANN).

The efficiency of various features and the combination of a hybrid feature set prove to be effective in extracting the features and classifying the two categories of images. Performance metric values like True Positive Rate, False Positive Rate, sensitivity, specificity, accuracy, and F1 Score were used to identify the efficiency of the classifier [26].

B. Confusion Matrix

In the confusion matrix: TP (True Positive) Predicts Cancerous as Cancerous, FP (False Positive) Predicts Cancerous as Normal, TN (True Negative) Predicts Normal as Normal, FN (False Negative) Predicts Normal as Cancerous, NPV denotes the Negative Predictive Value, PPV denotes the Positive Predictive Value. Sensitivity and specificity are the proportions of positive and negative cases, respectively. The classifier showed that both the parameters had shown outperforming results. The final result proves that the classifier performs better in classifying the required categories. The confusion matrix is plotted for the proposed algorithm.

The parameters considered for comparison are Positive Predictive Value (Precision), Negative Predictive Value, Sensitivity (Recall), Specificity, Accuracy, and F1-Score of different classifiers. The Positive Predictive value or Precision for the ANFIS model is 99.5%, indicating that the positive prediction is best in the maximum of the iterations. The Negative predictive value is 98% in LDA, proving that it rarely misclassifies the negative cases. When the overall accuracy is considered, which combines both positives and negatives, the Proposed ANFIS model again ranks highest at 97.3%, showing it has the most reliable overall classification performance[27][28]. The F1-Score value obtained using the proposed algorithm is 0.9686, which interprets to be better as there is no major deviation as the perfect value ranges till 1. F1 Score=0.9787.

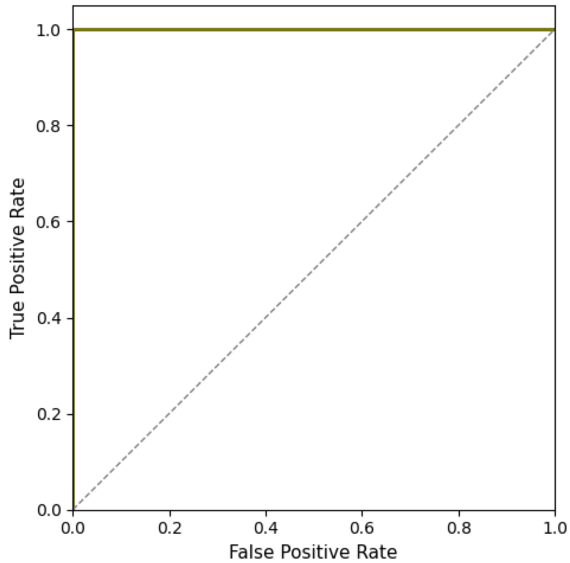

Fig. 6. Receiver Operating Characteristic Curve

In evaluating the performance of uterine MRI image classification, various metrics, such as True Positive Rate, False Positive Rate, sensitivity, specificity, accuracy, and F1 Score, are considered. Among these, the F1 Score emerges as a particularly pertinent metric for decision-making in this context, offering a balanced

Manuscript received 22November 2024; Revised 10 March 2025; 10 June 2025; Accepted 15 July 2025; Available online 30July 2025
Digital Object Identifier (**DOI**): https://doi.org/10.35882/jeeemi.v7i3.632

assessment of a classifier's precision and recall, crucial in medical image classification tasks with class imbalances. Computed as the harmonic mean of precision and recall, the F1 Score measures of the classifier's overall effectiveness. Its significance lies in its ability to address both false positives and false negatives, making it a comprehensive metric for gauging the classifier's utility in clinical applications. Shifting focus to endometrial carcinoma classification, the ROC curve, depicted in Fig.6, reveals an impressive Area Under the Curve (AUC) of 0.97 for the Adaptive Neuro-Fuzzy Inference System (ANFIS) Classifier. This underscores the model's proficiency in distinguishing between normal and abnormal endometrial cases, striking a balance between True Positive Rate (TPR) and False Positive Rate (FPR). The calculated F1 Score of 0.9787 further accentuates the precision and sensitivity of the ANFIS Classifier in specifically classifying endometrial carcinoma cases. These results collectively emphasize the robust performance of the classifier, positioning it as a promising tool for accurate and reliable endometrial carcinoma classification in clinical practice. This implies that the ANFIS Classifier is not only proficient in correctly identifying cases of endometrial carcinoma but also excels in minimizing the risk of false positives, a crucial consideration in medical applications where misclassification can have significant consequences. Consequently, the combined evaluation of the F1 Score and ROC curve suggests that the ANFIS Classifier holds promise for reliable and accurate classification of endometrial carcinoma cases, demonstrating robust performance in both sensitivity and specificity[29].

To enhance the interpretability of our machine learning classifiers, Explainable AI (XAI) techniques are integrated into our MR imaging-based uterine cancer prediction system. This integration is pivotal for clinicians and patients alike, as it facilitates understanding and trust in the AI-driven decision-making process. XAI, specifically through layer-wise relevance propagation (LRP), justifies the model's predictions by mapping the output decisions back to the input features. The model uses a hybrid feature set from GLCM and GLRLM to state the cancer presence accurately. Through LRP, we provide a visualization that illuminates each feature's contribution to the final prediction, strengthening the importance of key features like entropy and contrast derived from GLCM and GLRLM. For example, in analyzing an abnormal MRI image, the XAI technique utilizes a heat map to showcase areas of concern, directly correlating to tumor presence with varying intensities. Contrarily, for standard imaging predictions, XAI reveals a pattern of uniform textures and intensities reflective of healthy tissue, which supports the non-cancerous classification made by the model. Integrating XAI techniques enables a more transparent and comprehensible AI model, bridging the gap between the model's high-level capabilities and the practical needs of medical professionals. The results clearly demonstrate the effectiveness of the proposed machine learning-based method for identifying uterine cancer using a hybrid feature set derived from GLCM and GLRLM texture properties. Through outstanding accuracy of 97.3%, sensitivity of 96.3%, and specificity of 99.2%, the Adaptive Neuro-Fuzzy Inference System (ANFIS) classifier outperformed conventional machine learning algorithms. These results validate the effectiveness of the normalization and ranking procedures used for feature selection and support the efficacy of texture-based features in identifying significant patterns related to endometrial carcinoma. Additionally, the model's predictions were simpler to comprehend because of the integration of Explainable AI (XAI), which connects the gap between clinical insights and computational outputs.

4. Conclusion

The aim of this research was to develop a soft computing-based system for accurate uterine cancer detection by classifying abnormal and normal medical images. The system utilized a hybrid feature set combining Gray-Level Co-occurrence Matrix (GLCM) and Gray-Level Run Length Matrix (GLRLM) features, with a novel feature selection approach to reduce complexity. The proposed Adaptive Neuro-Fuzzy Inference System (ANFIS) classifier outperformed six other machine learning classifiers, achieving an accuracy of 97.3%, sensitivity of 96.3%, and specificity of 99.2% when tested on 1,398 image samples. The positive and negative prediction accuracies were 95.5% and 93.4%, respectively, with an F1 score of 0.9787. Type-I and Type-II errors were minimal, with 17 and 2 images misclassified, respectively. The ROC curve indicated strong performance. Future work could focus on optimizing feature selection, testing on larger and more diverse datasets, exploring hybrid classifiers, and real-time clinical application of the system.

Acknowledgment

The authors sincerely thank Avinashilingam Institute for Home Science and Higher Education for Women and Nandha Engineering College for their support and encouragement throughout the research. We also extend our gratitude to the journal's editorial and review team for their insightful comments and suggestions to enhance this work.

References:

[1] N. Sriraam and L. Vinodashri, “A Computer Aided Diagnostic Tool for the Detection of Uterine

Manuscript received 22November 2024; Revised 10 March 2025; 10 June 2025; Accepted 15 July 2025; Available online 30July 2025
Digital Object Identifier (DOI): https://doi.org/10.35882/jeeemi.v7i3.632

Fibroids," *Int. J. Biomed. Clin. Eng.*, vol. 2, no. 1, pp. 26–38, Jan. 2013, doi: 10.4018/ijbce.2013010103.

[2] Z. A. Al-Saffar and T. Yildirim, "A Novel Approach to Improving Brain Image Classification Using Mutual Information-Accelerated Singular Value Decomposition," *IEEE Access*, vol. 8, pp. 52575–52587, 2020, doi: 10.1109/ACCESS.2020.2980728.

[3] Z.-Y. Wei, Z. Zhang, D.-L. Zhao, W.-M. Zhao, and Y.-G. Meng, "Magnetic resonance imaging-based radiomics model for preoperative assessment of risk stratification in endometrial cancer," *World J. Clin. Cases*, vol. 12, no. 26, pp. 5908–5921, 2024, doi: 10.12998/wjcc.v12.i26.5908.

[4] J. N. B.-G. B. Long, M. A. Clarke, A. D. M. Morillo, N. Wentzensen, *Ultrasound detection of endometrial cancer in women with postmenopausal bleeding: Systematic review and meta-analysis*, vol. 157, no. 3. 2020. doi: https://doi.org/10.1016/j.ygyno.2020.01.032.

[5] V. Chiappa *et al.*, "Using Radiomics and Machine Learning Applied to MRI to Predict Response to Neoadjuvant Chemotherapy in Locally Advanced Cervical Cancer," *Diagnostics*, vol. 13, no. 19, pp. 0–11, 2023, doi: 10.3390/diagnostics13193139.

[6] Yanyan Yua · Xingqing Qina · Yongmei Huanga · Jinyuan Liao Yuanfang Taoa,1 · Yuchen Weia, "Development and Validation of a Nomogram Based on Multiparametric MRI for Predicting Lymph Node Metastasis in Endometrial Cancer: A Retrospective Cohort Study," *Acad. Radiol.*, vol. Volume 32, no. 5, pp. 2751–2762, 2024, doi: 10.1016/j.acra.2024.12.008.

[7] G. Nallasivan, M. Vargheese, J. Banukumar, and A. Ahila, "An Automated and Improved Brain Tumor Detection in Magnetic Resonance Images," vol. 12, no. 11, pp. 3370–3378, 2021.

[8] J. Liu and Z. Wang, "Advances in the Preoperative Identification of Uterine Sarcoma," *Cancers (Basel).*, vol. 14, no. 14, pp. 1–15, 2022, doi: 10.3390/cancers14143517.

[9] B. J. 1 Xueliang Zhu 1, Jie Ying 2, Haima Yang 1, Le Fu 3, Boyang Li 1, "Detection of deep myometrial invasion in endometrial cancer MR imaging based on multi-feature fusion and probabilistic support vector machine ensemble," *Comput. Biol. Med.*, vol. Jul;134:10, no. May 11, 2021, doi: 10.1016/j.compbiomed.2021.104487.

[10] G. L. A *et al.*, "Machine learning for prediction of concurrent endometrial carcinoma in patients diagnosed with endometrial intraepithelial neoplasia," *Eur. J. Surg. Oncol.*, vol. Volume 50, no. Issue 3, p. 108006, 2024, doi: https://doi.org/10.1016/j.ejso.2024.108006.

[11] Y. Zhang, C. Gong, L. Zheng, X. Li, and X. Yang, "Deep Learning for Intelligent Recognition and Prediction of Endometrial Cancer," *J. Healthc. Eng.*, vol. 2021, 2021, doi: 10.1155/2021/1148309.

[12] T. Y. 2 Masatoyo Nakajo 1, Megumi Jinguji 2, Atsushi Tani 2, Erina Yano 2, Chin Khang Hoo 2, Daisuke Hirahara 3, Shinichi Togami 4, Hiroaki Kobayashi 4, "Machine learning based evaluation of clinical and pretreatment 18F-FDG-PET/CT radiomic features to predict prognosis of cervical cancer patients," *Abdom. Radiol.*, vol. 47, no. Nov., pp. 838–847, 2021, doi: 10.1007/s00261-021-03350-y.

[13] S. O. A *et al.*, "Radiomic machine learning for pretreatment assessment of prognostic risk factors for endometrial cancer and its effects on radiologists' decisions of deep myometrial invasion," *Magn. Reson. Imaging,* vol. 85, pp. 161–167, 2022, doi: https://doi.org/10.1016/j.mri.2021.10.024.

[14] P. P. Mainenti *et al.*, "MRI radiomics: A machine learning approach for the risk stratification of endometrial cancer patients," *Eur. J. Radiol.*, vol. 149, no. September 2021, p. 110226, 2022, doi: 10.1016/j.ejrad.2022.110226.

[15] Z. et al. Huang, ML., Ren, J., Jin, "Application of magnetic resonance imaging radiomics in endometrial cancer: a systematic review and meta-analysis.," *Radiol med*, vol. 129, pp. 439–456, doi: https://doi.org/10.1007/s11547-024-01765-3.

[16] J. S. A *et al.*, "Gynecological cancer prognosis using machine learning techniques: A systematic review of the last three decades," *Artif. Intell. Med.*, vol. Volume 139, no. May, p. 102536, 2023, doi: https://doi.org/10.1016/j.artmed.2023.102536.

[17] S. Shanmugam and S. Dharmar, "Very large scale integration implementation of seizure detection system with on-chip support vector machine classifier," *IET Circuits, Devices Syst.*, vol. 16, no. 1, pp. 1–12, 2022, doi: 10.1049/cds2.12077.

[18] S. Brindha and J. Justin, "Comparative Analysis on De-Noising of MRI Uterus Image for Identification of Endometrial Carcinoma," *Front. Biomed. Technol.*, vol. 10, no. 3, pp. 299–307, 2023, doi: 10.18502/fbt.v10i3.13159.

[19] D. C. Rini Novitasari, A. Lubab, A. Sawiji, and A. H. Asyhar, "Application of feature extraction for breast cancer using one order statistic, glcm, glrlm, and gldm," *Adv. Sci. Technol. Eng. Syst.*,

Manuscript received 22November 2024; Revised 10 March 2025; 10 June 2025; Accepted 15 July 2025; Available online 30July 2025
Digital Object Identifier (**DOI**): https://doi.org/10.35882/jeeemi.v7i3.632

vol. 4, no. 4, pp. 115–120, 2019, doi: 10.25046/aj040413.

[20] M. P. 1 Carolina Bezzi 1 2, Alice Bergamini 1 3, Gregory Mathoux 4, Samuele Ghezzo 1 2, Lavinia Monaco 4, Giorgio Candotti 3, Federico Fallanca 2, Ana Maria Samanes Gajate 2, Emanuela Rabaiotti 3, Raffaella Cioffi 3, Luca Bocciolone 3, Luigi Gianolli 2, GianLuca, "Role of Machine Learning (ML)-Based Classification Using Conventional 18F-FDG PET Parameters in Predicting Postsurgical Features of Endometrial Cancer Aggressiveness," *Cancers (Basel).*, vol. 15, no. 1, p. 325, 2023, doi: doi: 10.3390/cancers15010325.

[21] H. Ganesan, Karthick & Rajaguru, "Performance analysis of KNN classifier with various distance metrics method for MRI images," *Soft Comput. Signal Process.*, p. pp 673–682, doi: DOI:10.1007/978-981-13-3600-3_64.

[22] W. L. a B, Q. G. c D, M. D. c E, W. C. F, and T. T. c G, "Multiclass diagnosis of stages of Alzheimer's disease using linear discriminant analysis scoring for multimodal data," *Comput. Biol. Med.*, vol. Volume 134, p. 104478, 2021, doi: https://doi.org/10.1016/j.compbiomed.2021.104478.

[23] C. M. A. K. Z. Basha, T. S. Teja, T. R. Teja, C. Harshita, and M. R. S. Sai, "Advancement in Classification of X-Ray Images Using Radial Basis Function with Support of Canny Edge Detection Model," *Comput. Vis. Bio-Inspired Comput.*, pp. 29–40., 2021, doi: DOI:10.1007/978-981-33-6862-0_3.

[24] S. Jayachitra and A. Prasanth, "Multi-Feature Analysis for Automated Brain Stroke Classification Using Weighted Gaussian Naïve Bayes Classifier," *J. Circuits, Syst. Comput.*, vol. 30, no. 10, 2021, doi: 10.1142/S0218126621501784.

[25] Virupakshappa and B. Amarapur, "Computer-aided diagnosis applied to MRI images of brain tumor using cognition based modified level set and optimized ANN classifier," *Multimed. Tools Appl.*, vol. 79, no. 5–6, pp. 3571–3599, 2020, doi: 10.1007/s11042-018-6176-1.

[26] R. Trevethan, "Sensitivity, Specificity, and Predictive Values: Foundations, Pliabilities, and Pitfalls in Research and Practice," *Front. Public Heal.*, vol. 5, no. November, pp. 1–7, 2017, doi: 10.3389/fpubh.2017.00307.

[27] B. Samarasam and J. Justin, "Enhanced Classification of Endometrial Carcinoma Using Machine Learning Powered by Explainable AI," *African J. Biomed. Res.*, vol. 28, no. 1, pp. 158–165, Jan. 2025.

[28] A. S. A and K. Manivannan, "Fusion based Glioma brain tumor detection and segmentation using ANFIS classification," *Comput. Methods Programs Biomed.*, vol. Volume 166, no. November, p. Pages 33-38, 2018, doi: https://doi.org/10.1016/j.cmpb.2018.09.006.

[29] I. Bajla and M. Teplan, "Yeast cell detection in color microscopic images using ROC-optimized decoloring and segmentation," *IET Image Process.*, vol. 16, no. 2, pp. 606–621, 2022, doi: 10.1049/ipr2.12376.

[30] Database: https://www.cancerimagingarchive.net/collections/captac-ucec/

Author Biography

Brindha Samarasam is a Research Scholar at the Avinashilingam Institute of Higher Education for Women and an Assistant Professor in the Department of Electronics and Communication Engineering at Nandha Engineering College, India. She holds a Bachelor's degree in Biomedical Instrumentation Engineering and a Master's in Applied Electronics. Her research focuses on medical image analysis, machine learning, Explainable AI (XAI), and cancer diagnostics, particularly in texture feature extraction using LBP, HOG, GLCM, and GLRLM techniques. She has authored 15 publications, held three patents, and serves as a reviewer for reputed journals. She has contributed to NAAC/NBA accreditation andactively engages in academic and social initiatives, including the Empower. Her camp and the Aram Sei social club. She has participated in 20+ national and international conferences and has an ORCID ID: 0000-0001-7632-0316.

Dr. Judith Justin is a Professor and Head of the Department of Biomedical Instrumentation Engineering at the School of Engineering, Avinashilingam Institute for Home Science and Higher Education for Women, Coimbatore, India. She earned her Bachelor's degree in Instrumentation and Control Engineering from the Government College of Technology, Coimbatore, and her Master's in Biomedical Engineering from the Indian Institute of Technology (IIT) Madras. Dr. Justin obtained her Ph.D. in Information and Communication Engineering from Anna University, Chennai. Her research interests include speech signal processing, biomedical instrumentation, and computational intelligence. She has published numerous research papers and has been actively involved in research supervision and academic leadership.

Manuscript received 22November 2024; Revised 10 March 2025; 10 June 2025; Accepted 15 July 2025; Available online 30July 2025
Digital Object Identifier (**DOI**): https://doi.org/10.35882/jeeemi.v7i3.632